RSC Advances

ROYAL SOCIETY OF CHEMISTRY

www.rsc.org/advances

Hypercrosslinked Microporous Polymers Based on Carbazole for Gas Storage and Separation

Xiao Yang, Miao Yu, Yang Zhao, Chong Zhang, Xiaoyan Wang, Jia-Xing Jiang*

School of Materials Science and Engineering, Shaanxi Normal University, Xi'an, 710062, Shaanxi, P. R. China

E-mail: jiaxing@snnu.edu.cn.

Abstract

Two hypercrosslinked microporous organic polymer networks from carbazole derivatives have been synthesized via Friedel-Crafts alkylation using a formaldehyde dimethyl acetal crosslinker promoted by anhydrous $FeCl_3$. Both of the polymer networks are stable in various solvents and thermally stable. The polymer network FCTCz produced from a dendritic carbazole building block shows much higher Brunauer-Emmet-Teller specific surface area of 1845 m^2 g^{-1} than the dicarbazolic polymer network of FCBCz (1067 m^2 g^{-1}). FCTCz exhibits a high carbon dioxide uptake ability of 4.63 mmol g^{-1} at 1.13 bar and 273 K with a hydrogen uptake ability of 1.94 wt% (1.13 bar/77 K). In addition, both of the polymer networks exhibit good ideal CO_2/N_2 selectivity (26–29) and CO_2/CH_4 selectivity (5.2–5.8) at 273 K. These results demonstrated that this kind of polymer networks is very promising candidates for potential applications in post-combustion carbon dioxide capture and sequestration technology.

Keywords: hypercrosslinked porous polymers; carbazole building blocks; gas storage; carbon dioxide capture; heat of sorption.

Introduction

Carbon capture and storage technologies (CCS) have been the subjects of intense resent interest since the excessive emission of carbon dioxide from the rapid consumption of fossil fuels leads to global climate change and some environment issues. Porous organic polymers (POPs) show great potential for carbon dioxide capture and separation due to their large specific surface area, high chemical and thermal stability, low regeneration energy, and synthetic diversity. The past decade has witnessed a rapid development of a wide variety of POPs, and the notable examples include polymers of intrinsic microporosity (PIMs),[1, 2] covalent organic frameworks (COFs),[3-5] conjugated microporous polymers (CMPs),[6-8] porous polymer networks (PPNs),[9] porous aromatic framework (PAFs),[10] covalent triazine-based frameworks (CTFs),[11] porous benzimidazolelinked polymers (BILPs),[12] and hypercrosslinked porous polymers (HCPs).[13-15]

As a subclass of porous organic polymers, HCPs could be facilely prepared on a large scale using a versatile route known as ‘‘knitting’’ method.[16] Applying this strategy, a wide range of aromatic monomers without specific polymerisable groups could be used to produce hypercrosslinked polymer networks with high porosity.[17] Therefore, the facile and cost-effective preparation processes make HCPs strong candidates for carbon capture and clean energy storage. For example, triphenylbenzene-based HCPs showed high surface areas up to 1059 $m^2 g^{-1}$ with a H_2 uptake capacity of 1.58 wt% (1.13 bar and 77 K),[16] tetraphenylethylene-based HCPs with a higher surface area of 1980 $m^2 g^{-1}$ exhibited the CO_2 uptake capacity of 3.63 mmol g^{-1} (1.0 bar and 273 K),[18] binaphthol-based HCPs showed an improved CO_2 uptake capacity as high as 3.96 mmol g^{-1} (1.0 bar and 273 K) because the incorporation of polar hydroxyl groups enhanced the interaction between the pore

wall and the CO_2 molecules.[19] In addition, it has been proved that carbazole and its derivatives are efficient building blocks to produce high surface area porous polymers with enhanced CO_2 capture performances. For example, the conjugated microporous polycarbazole showed a high surface area of 2220 m^2 g^{-1} with a CO_2 uptake capacity of 4.82 mmol g^{-1} (1.13 bar and 273 K),[20] the conjugated microporous network of P2 with carbazole–spacer–carbazole topological model structure and hydroxyl groups exhibited a CO_2 uptake capacity of 14.5 wt% (~3.29 mmol g^{-1}) at 1.13 bar and 273 K,[21] the carbazolic porous organic framework of Cz-POF-3 from a branched carbazole building block gave rise to a high CO_2 uptake capacity of 21.0 wt% (~4.77 mmol g^{-1}) at 1.13 bar and 273 K,[22] and the task-specific porous organic polymer TSP-2 with carbazole and triazine groups showed a CO_2 uptake capacity of 4.1 mmol g^{-1} at 1 bar and 273 K.[23] These results demonstrated that such carbazole-functionalized MOPs have great potential to increase the CO_2 capture capacity.

With this in mind, we synthesized two hypercrosslinked microporous organic polymer networks from dicarbazole and tricarbazole building blocks via Friedel-Crafts alkylation promoted by anhydrous $FeCl_3$. We expect that the surface area of the resulting polymer networks could be improved by using a dendritic carbazole building block with high connectivities of carbazole unit and, on the other hand, the nitrogen-rich polymer networks can enhance the binding affinity between the polymer adsorbent and carbon dioxide which results in the increase of carbon dioxide capture capacity.

Results and Discussion

The polymer networks were synthesized via Friedel-Crafts alkylation using a formaldehyde dimethyl acetal crosslinker promoted by anhydrous $FeCl_3$.[24] Scheme 1

shows the general synthetic routes for the two porous polymer networks. Reaction of 1,4-bis(carbazol-9yl)benzene (M1) or 1,3,5-tri(9H-carbazol-9-yl)benzene (M2) catalyzed by anhydrous $FeCl_3$ gave the carbazolic polymer networks of FCBCz and FCTCz, respectively. Yields of the polymer networks were quantitative, as observed for most other reported HCPs.[16, 18, 25] We need to point out that the polymer structure for the resulting polymer networks should be much more complicated than that shown in Scheme 1, since carbazole monomers could take place homo-coupling polymerization under the reaction conditions employed in this work.[20, 22] Therefore, the resulting polymer networks might consist of the homocoupled polymer from carbazole monomers themselves and the crosslinked polymer network with crosslinker of FDA. Both of the two polymers are insoluble in conventional organic solvents because of their highly crosslinked structures and they are also chemically stable. The FT-IR spectra of the polymer networks (Fig. *S1*) were consistent with the excepted network structures showing the unsaturated C=C vibration bands at 1500 and 1650 cm^{-1}, the C-H stretching vibrations originating from $–CH_2–$ at 2930 cm^{-1}, and the weak band at 1350 cm^{-1} is attributed to the stretching vibration of C-N-C.[25] The resulting polymer networks are thermally stable in nitrogen atmosphere up to 350 ^{0}C as revealed by TGA (Fig. *S2*), and retain more than 65% of the mass even at 800 ^{0}C. Powder X-ray diffraction measurements indicated that the polymer networks are amorphous in nature (Fig. *S3*), as for most other reported HCPs networks.[13, 16, 18, 26] Electron microscopy images indicated that FCBCz shows spherical nanobeads, while FCBCz consists of irregular solid sub-micron particles (Fig. *S4*).

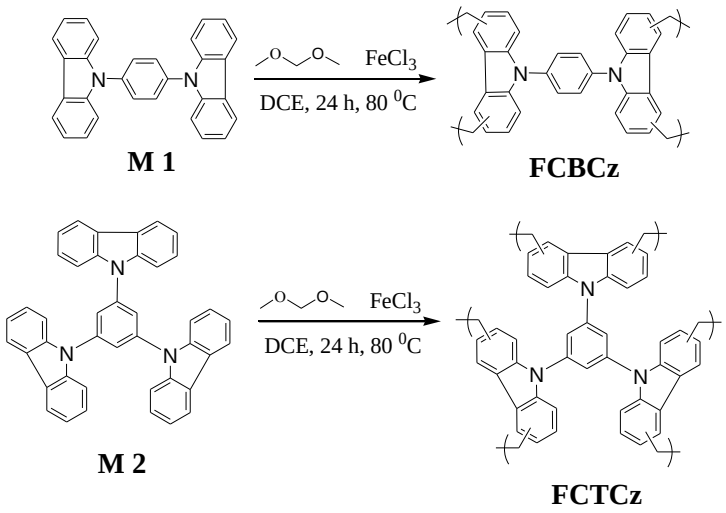

Scheme 1. Synthetic routes to the polymer networks and the notional polymer structures.

The porous properties of the both polymer networks were investigated by nitrogen adsorption analyses at 77.3 K. As shown in Fig. 1a, the polymer network of FCBCz gave rise to a typical Type I nitrogen gas sorption isotherm with a steep nitrogen gas uptake at low relative pressure ($P/P_0 < 0.001$), indicating that it is a typical microporous material, while the polymer network of FCTCz showed broadly a Type II nitrogen gas sorption isotherm in nature with evidence of some Type IV character showing a steep rise in the nitrogen adsorption at high relative pressures ($P/P_0 > 0.9$), indicating the presence of some mesopores and/or macropores in the network as well, which are probably due to inter-particle porosity or void.[20, 27] In addition, significant hysteresis was also observed in desorption branch for FCTCz, which is consistent with elastic deformations or swelling as a result of gas sorption.[28] Fig. 1b shows the pore size distribution (PSD) curves for the two polymer networks as calculated using nonlocal density functional theory (NL-DFT). FCBCz exhibits a median micropore diameter of 0.89 nm with a shoulder peak around at 1.54 nm, while FCTCz shows a slight bigger micropore diameter centered at around 0.98 nm and a shoulder peak located at 1.58 nm with a spot mesopores peaked at around 2.12 and 4.95 nm, indicating that FCTCz has bigger micropore size and many more mesopores

than FCBCz, which is in line with the nitrogen adsorption-desorption isotherms. The apparent BET surface areas were found to be 1067 and 1845 $m^2 g^{-1}$ for FCBCz and FCTCz, respectively. Compared to FCBCz, FCTCz shows much higher surface area, which could be attributed to the more active connectivities from the dendritic carbazole building block (M2) promoting the efficiency of cross-polymerization.[22] It is noteworthy that the surface areas for both of the polymer networks are higher than those of the HCPs reported by Han *et. al.*[24] (*e.g.* FCBCz: 1067 $m^2 g^{-1}$ *vs* CPOP-13: 890 $m^2 g^{-1}$; FCTCz: 1845 $m^2 g^{-1}$ *vs* CPOP-15: 1190 $m^2 g^{-1}$), the possible reason is that much more formaldehyde dimethyl acetal crosslinker (the molar ratio of monomer : FDA = 1:4 for FCBCz, and 1:6 for FCTCz because of the different active sites of the monomers) and longer reaction time of 24 h were employed in this work than those in Han's work, where the molar ratio of monomer : FDA was 1:1 and reaction time was 12 h.[24] These promoted the crosslinked degree of the formed polymer networks and the completion of polymerization, which lead to the improvement of surface area, as observed for other HCPs produced by using the similar experiment procedures.[16] The micropore surface areas derived using the t-plot method were 892 and 1074 $m^2 g^{-1}$ for FCBCz and FCTCz, respectively. The total pore volumes, estimated from the amount of gas adsorbed at P/P_o = 0.98, were 0.71 and 2.91 $cm^3 g^{-1}$, while the micropore volumes derived from cumulative pore volume graph were 0.43 and 0.51 $cm^3 g^{-1}$ for FCBCz and FCTCz, respectively. These results again demonstrated a significant proportion of mesopores in FCTCz (Table 1). The surface area of 1845 $m^2 g^{-1}$ for FCTCz is comparable to that of the other reported HCPs, such as the carbazolic porous organic frameworks (S_{BET} = 2065 $m^2 g^{-1}$),[22] the tetraphenylethylene-based HCPs (S_{BET} = 1980 $m^2 g^{-1}$),[18] the tetraphenylmethane-based HCPs (S_{BET} = 1679 $m^2 g^{-1}$),[29] and much higher than that of the benzene-based HCPs

(S_{BET} = 1391m^2 g^{-1}),[16] the binaphthol-based HCPs (S_{BET} = 1015 m^2 g^{-1}),[19] and the task-specific porous organic polymer TSP-2 bifunctionalized with carbazole and triazine groups (S_{BET} = 913 m^2 g^{-1}).[23]

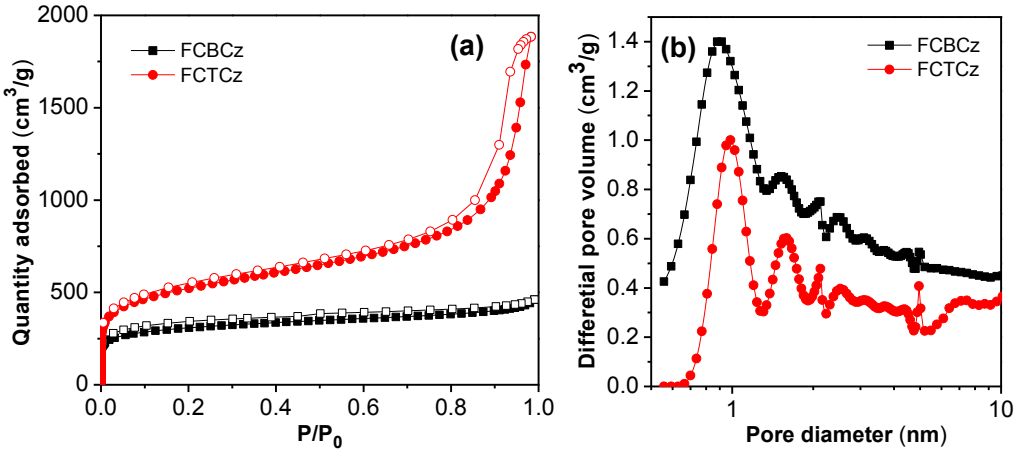

Fig. 1 a) Nitrogen adsorption/desorption isotherms for the polymer networks (the adsorption branch is labeled with filled symbols and desorption branch is labeled with open symbols); b) Pore size distribution curves calculated by NL-DFT.

Table 1 Summary of pore properties for the polymer networks

Polymer	S_{BET} [a] [m^2/g]	S_{Micro} [b] [m^2/g]	V_{Micro} [c] [cm^3 g^{-1}]	V_{Total} [d] [cm^3 g^{-1}]	S_{Micro}/S_{BET} [%]	V_{Micro}/V_{Total} [%]
FCBCz	1067	892	0.43	0.71	83.60	60.56
FCTCz	1845	1074	0.51	2.91	58.21	17.53

[a] Surface area calculated from N_2 adsorption isotherm in the relative pressure (*P/Po*) range from 0.05 to 0.20; [b] Micropore surface area calculated from the N_2 adsorption isotherm using t-plot method based on the Harkins Jura Equation. [c] The micropore volume derived from the t-plot method; [d] Total pore volume at *P/Po* = 0.98.

Such microporous polymer networks, with the virtue of the high specific surface area, small pore size, and high nitrogen content, may interact selectively with certain gas molecules, thus inspiring us to investigate their gas uptake capacities. Fig. 2a shows the volumetric hydrogen sorption curves of the two polymer networks at 77.3 K up to a pressure of 1.13 bar. The polymer network of FCTCz, possessing higher micropore surface area and micropore volume (Table 1), exhibits higher hydrogen uptake ability of 218 cm^3 g^{-1} (~1.94 wt%) than that of FCBCz (175 cm^3 g^{-1}, ~1.56

wt%) at 77 K/1.13 bar. The hydrogen uptake capacity of FCTCz is higher than that of some previously reported HCPs under the same conditions, such as the benzene-based HCPs (1.45 wt%),[16] the heterocyclic-based HCPs (1.58 wt%),[30] the tetraphenylethylene-based HCPs (1.76 wt%),[18] and the benzenedimethanol-based HCP-BDM (1.11 wt%),[31] although it is lower than that of the carbazole-based CMP (2.80 wt%)[20] and the carbazolic porous organic frameworks Cz-POF-1 (2.24 wt%)[22] at 77 K and 1.13 bar.

The CO_2 uptakes of the polymer networks were measured up to 1.13 bar at 273 and 298 K, respectively (Fig. 2b). FCTCz shows a higher CO_2 capture capacity of 4.63 mmol g^{-1} than FCBCz (3.61 mmol g^{-1}) at 1.13 bar/273 K, which could be attributed to the higher micropore surface area, micropore volume, and nitrogen content for FCTCz. The CO_2 uptake of 4.63 mmol g^{-1} for FCTCz lies towards the upper end when compared to other HCPs under the same conditions, such as the carbazolic porous organic frameworks (4.77 mmol g^{-1}),[22] the triazine-based TSP-2 (4.10 mmol g^{-1}),[23] the tetraphenylethylene-based HCPs (3.63 mmol g^{-1}),[18] the triphenylbenzene-based HCPs (3.61 mmol g^{-1}),[16] the binaphthol-based BINOL (3.96 mmol g^{-1}),[19] and much higher than that of the tetraphenylmethane-based HCPs (2.27 mmol g^{-1}),[29] the polythiophene-based Th-1 (2.89 mmol g^{-1}),[30] the benzenedimethanol-based HCP-BDM (2.86 mmol g^{-1}),[31] and the conjugated microporous polymers (1.80–3.86 mmol g^{-1}) with much higher surface areas,[32] but still lower than that of the imine-linked porous polymer frameworks (*e.g.* 6.1 mmol g^{-1} for PPF-1).[33] The high CO_2 capture property of FCTCz might arise from the high surface area and the dipole-quadrupole interactions between the electro-rich nitrogen atoms and the electro poorer carbon dioxide molecules.

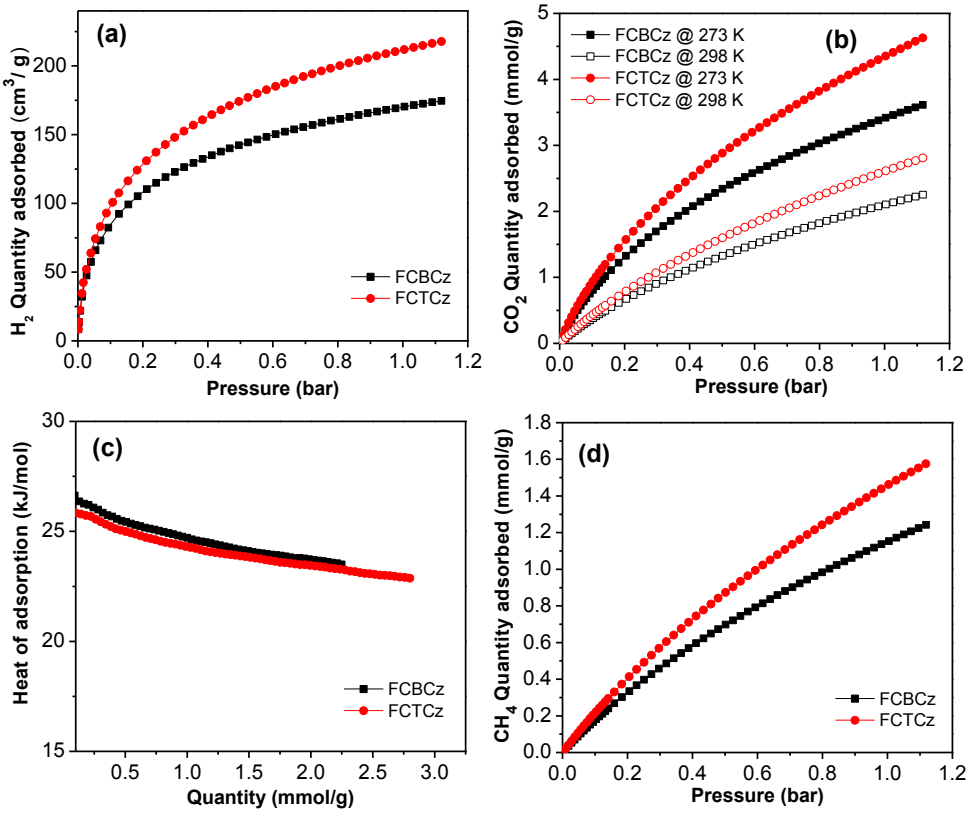

Fig. 2 a) Volumetric H_2 sorption curves for the polymer networks at 77.3 K up to 1.13 bar; b) CO_2 adsorption isotherms for the polymer networks at 273 K and 298 K, respectively; c) Isosteric heats of adsorption for CO_2 calculated from the adsorption isotherms collected at 273 K and 298 K; d) CH_4 adsorption isotherms for the polymer networks at 273 K.

To provide a better understanding of the CO_2 capture properties, the isosteric heat of adsorption (Q_{st}) was calculated from the Clausius–Clapeyron equation using the CO_2 adsorption data collected at 273 K and 298 K. As shown in Fig. 2c, both of the polymer networks show high isosteric heats of CO_2 adsorption over 26 kJ mol^{-1}. FCBCz shows a slight higher Q_{st} (27.09 kJ mol^{-1}) than FCTCz (26.38 kJ mol^{-1}) at the zero-coverage, which could be attributed to the smaller micropore size of FCBCz than FCTCz as discussed above, and small pore sizes known to increase the heat of adsorption.[34] However, as the lower surface area and pore volume, FCBCz shows less CO_2 adsorption (3.61 mmol g^{-1}) than FCTCz (4.63 mmol g^{-1}) at 273 K/1.13 bar. In addition, these Q_{st} values are higher than those of the benzene-based HCPs (21.2–23.5 kJ mol^{-1}),[26] and can be comparable to those of the porous benzimidazole-linked

polymers (26.7–28.8 kJ mol^{-1}),[35] the carbazolic porous organic frameworks (24.8–27.8 kJ mol^{-1}),[22] and some functionalized CMP materials (25–33 kJ mol^{-1}).[32] However, the heats of absorption for the networks still remain below the energy of chemisorptive processes (>40 kJ mol^{-1}),[36] indicating strong interactions between the nitrogen-rich polymer networks and the polarizable CO_2 molecules through dipole-quadrupole interactions, and also the inherent microporosity of the polymer networks which is more favourable for CO_2 desorption.

Table 2 Gas uptakes for the polymer networks

Polymer	H_2 uptake [a] [wt%]	CH_4 uptake [b] [mmol g^{-1}]	CO_2 uptake [b] [mmol g^{-1}]	CO_2 uptake [c] [mmol g^{-1}]	Selectivity [d]	
					CO_2/CH_4	CO_2/N_2
FCBCz	1.56	1.24	3.61	2.25	5.8	28.9
FCTCz	1.94	1.58	4.63	2.81	5.2	26.1

[a] Data were obtained at 1.13 bar and 77.3 K; [b] Data were obtained at 1.13 bar and 273 K; [c] Data were obtained at 1.13 bar and 298 K. [d] Adsorption selectivity based on the Henry's law.

The methane sorption performance of the polymer networks was also explored (Fig. 2d). As expected, the polymer network of FCTCz with higher surface area and micropore volume exhibits higher methane uptake ability of 1.58 mmol g^{-1} than FCBCz (1.24 mmol g^{-1}) at 273 K/1.13 bar (Table 1). This value is comparable to that of the carbazole–spacer–carbazole based conjugated microporous polymers (1.35~2.00 mmol g^{-1})[21] and the carbazolic porous organic frameworks (POFs) (0.63~1.56 mmol g^{-1})[22] under the same condition. In order to investigate the gas adsorption selectivity of the microporous polymer networks, CO_2, N_2, and CH_4 sorption properties were measured by volumetric methods at the same conditions (Fig. *S5 & S6*). The selectivity was estimated using the ratios of the Henry's law constants calculated from the initial slopes of the single-component gas adsorption isotherms at low pressure coverage (< 0.15 bar). The calculated CO_2/CH_4 adsorption selectivities were about 5.8 and 5.2 for FCBCz and FCTCz at 273 K, respectively. The

selectivities are comparable to those of some reported POPs, such as the carbazole–spacer–carbazole based CMPs with the CO_2/CH_4 selectivity of 4,[21] the carbazolic porous organic frameworks (4.4–4.7 for Cz-POF1–3),[22] although they are lower than those of the porous benzimidazole-linked polymers (8–17).[35] The calculated CO_2/N_2 adsorption selectivities were 28.9 and 26.1 for FCBCz and FCTCz at 273 K, respectively. Though these values are lower than those of some other reported HCPs with the selectivity higher than 100, such as the pyrrole-based HCPs (117 for Py-1),[30] the tetraphenylethylene-based HCPs (119 for Network-7),[18] FCTCz shows much higher CO_2 adsorption capacity (Py-1, 2.7 mmol g^{-1}; Network-7, 1.92 mmol g^{-1}) and better CO_2/N_2 adsorption selectivity than that of many other type POPs.[33, 37, 38] Ideally, high CO_2 uptake and CO_2/N_2 adsorption selectivity are both required for practical applications. As such, the high CO_2 uptake capacity and the high adsorption selectivity for CO_2 over N_2 by these polymer networks make them promising candidates for applications in post-combustion CO_2 capture and sequestration technology.

Conclusions

In summary, two hypercrosslinked microporous organic polymer networks from carbazole building blocks have been synthesized via Friedel-Crafts alkylation using a formaldehyde dimethyl acetal crosslinker promoted by anhydrous $FeCl_3$. The polymer network FCTCz produced from the high active connectivities carbazole building blocks shows highly specific surface area up to 1845 m^2 g^{-1} with a high CO_2 uptake ability of 4.63 mmol g^{-1} (1.13 bar/273 K), and a high hydrogen uptake ability of 1.94 wt% (1.13 bar/77 K). Both of the polymer networks show high isosteric heats of CO_2 adsorption and good ideal CO_2/N_2 and CO_2/CH_4 selectivities. Considering the high surface area, the outstanding CO_2 sorption performances, and the facile preparation

strategy, these polymer networks are promising materials for potential applications in post-combustion CO_2 capture and separation.

Supporting Information

Electronic supplementary information (ESI) available: Experimental procedures, FT-IR, TGA, SEM images, and gas adsorption for the polymer networks. See DOI: 10.1039/XXXXX.

Acknowledgements

This work was supported by the National Natural Science Foundation of China (21304055), Research Fund for the Doctoral Program of Higher Education of China (20120202120007), Science and Technology Program of Shaanxi Province (2013KJXX-72), Shaanxi Innovative Team of Key Science and Technology (2013KCT-17), and the Fundamental Research Funds for the Central Universities (GK201103001, GK201101003 & GK201301002).

Notes and references

1. P. M. Budd, B. S. Ghanem, S. Makhseed, N. B. McKeown, K. J. Msayib and C. E. Tattershall, *Chem. Commun.*, 2004, 230-231.
2. N. B. McKeown and P. M. Budd, *Macromolecules*, 2010, **43**, 5163-5176.
3. A. P. Côté, A. I. Benin, N. W. Ockwig, M. O'Keeffe, A. J. Matzger and O. M. Yaghi, *Science*, 2005, **310**, 1166-1170.
4. H. M. El-Kaderi, J. R. Hunt, J. L. Mendoza-Cortes, A. P. Côté, R. E. Taylor, M. O'Keeffe and O. M. Yaghi, *Science*, 2007, **316**, 268-272.
5. S. Y. Ding and W. Wang, *Chem. Soc. Rev.*, 2013, **42**, 548-568.
6. J. X. Jiang, F. Su, A. Trewin, C. D. Wood, N. L. Campbell, H. Niu, C. Dickinson, A. Y. Ganin, M. J. Rosseinsky, Y. Z. Khimyak and A. I. Cooper, *Angew. Chem. Int. Ed.*, 2007, **46**, 8574-8578.
7. A. I. Cooper, *Adv. Mater.*, 2009, **21**, 1291-1295.
8. Y. Xu, S. Jin, H. Xu, A. Nagai and D. Jiang, *Chem. Soc. Rev.*, 2013, **42**, 8012-8031.
9. D. Yuan, W. Lu, D. Zhao and H. C. Zhou, *Adv. Mater.*, 2011, **23**, 3723-3725.
10. T. Ben, H. Ren, S. Ma, D. Cao, J. Lan, X. Jing, W. Wang, J. Xu, F. Deng, J. M. Simmons, S. Qiu and G. Zhu, *Angew. Chem. Int. Ed.*, 2009, **48**, 9457-9460.
11. P. Kuhn, M. Antonietti and A. Thomas, *Angew. Chem. Int. Ed.*, 2008, **47**, 3450-3453.
12. M. G. Rabbani and H. M. El-Kaderi, *Chem. Mater.*, 2011, **23**, 1650-1653.

13. J. Y. Lee, C. D. Wood, D. Bradshaw, M. J. Rosseinsky and A. I. Cooper, *Chem. Commun.*, 2006, 2670-2672.
14. J. Germain, J. Hradil, J. M. J. Fréchet and F. Svec, *Chem. Mater.*, 2006, **18**, 4430-4435.
15. M. P. Tsyurupa and V. A. Davankov, *React. Funct. Polym.*, 2006, **66**, 768-779.
16. B. Li, R. Gong, W. Wang, X. Huang, W. Zhang, H. Li, C. Hu and B. Tan, *Macromolecules*, 2011, **44**, 2410-2414.
17. S. Xu, Y. Luo and B. Tan, *Macromol. Rapid Commun.*, 2013, **34**, 471-484.
18. S. Yao, X. Yang, M. Yu, Y. Zhang and J.-X. Jiang, *J. Mater. Chem. A*, 2014, **2**, 8054-8059.
19. R. Dawson, L. A. Stevens, T. C. Drage, C. E. Snape, M. W. Smith, D. J. Adams and A. I. Cooper, *J. Am. Chem. Soc.*, 2012, **134**, 10741-10744.
20. Q. Chen, M. Luo, P. Hammershoj, D. Zhou, Y. Han, B. W. Laursen, C. G. Yan and B. H. Han, *J. Am. Chem. Soc.*, 2012, **134**, 6084-6087.
21. S. Qiao, Z. Du and R. Yang, *J. Mater. Chem. A*, 2014, **2**, 1877-1885.
22. X. Zhang, J. Lu and J. Zhang, *Chem. Mater.*, 2014, **26**, 4023-4029.
23. X. Zhu, S. M. Mahurin, S. H. An, C. L. Do-Thanh, C. Tian, Y. Li, L. W. Gill, E. W. Hagaman, Z. Bian, J. H. Zhou, J. Hu, H. Liu and S. Dai, *Chem. Commun.*, 2014, **50**, 7933-7936.
24. During the preparation of this manuscript, a similar study was reported by Han and co-workers: J.-H. Zhu, Q. Chen, Z.-Y. Sui, L. Pan, J. Yu and B.-H. Han, *J. Mater. Chem. A*, 2014, **2**, 16181-16189.
25. R. Dawson, T. Ratvijitvech, M. Corker, A. Laybourn, Y. Z. Khimyak, A. I. Cooper and D. J. Adams, *Polym. Chem.*, 2012, **3**, 2034-2038.
26. C. F. Martín, E. Stöckel, R. Clowes, D. J. Adams, A. I. Cooper, J. J. Pis, F. Rubiera and C. Pevida, *J. Mater. Chem.*, 2011, **21**, 5475-5483.
27. J. Weber, J. Schmidt, A. Thomas and W. Böhlmann, *Langmuir*, 2010, **26**, 15650-15656.
28. J. Weber, M. Antonietti and A. Thomas, *Macromolecules*, 2008, **41**, 2880-2885.
29. X. Jing, D. Zou, P. Cui, H. Ren and G. Zhu, *J. Mater. Chem. A*, 2013, **1**, 13926.
30. Y. Luo, B. Li, W. Wang, K. Wu and B. Tan, *Adv. Mater.*, 2012, **24**, 5703-5707.
31. Y. Luo, S. Zhang, Y. Ma, W. Wang and B. Tan, *Polym. Chem.*, 2013, **4**, 1126-1131.
32. R. Dawson, E. Stockel, J. R. Holst, D. J. Adams and A. I. Cooper, *Energy Environ. Sci.*, 2011, **4**, 4239-4245.
33. Y. Zhu, H. Long and W. Zhang, *Chem. Mater.*, 2013, **25**, 1630-1635.
34. F. Svec, J. Germain and J. M. J. Frechet, *Small*, 2009, **5**, 1098-1111.
35. M. G. Rabbani and H. M. El-Kaderi, *Chem. Mater.*, 2012, **24**, 1511-1517.
36. H. A. Patel, S. Hyun Je, J. Park, D. P. Chen, Y. Jung, C. T. Yavuz and A. Coskun, *Nat. Commun.*, 2013, **4**, 1357-1361.
37. X. Yang, S. Yao, M. Yu and J.-X. Jiang, *Macromol. Rapid Commun.*, 2014, **35**, 834-839.
38. Z. G. Wang, X. Liu, D. Wang and J. Jin, *Polym.Chem.*, 2014, **5**, 2793-2800.

Table of Content

Hypercrosslinked microporous polymers from carbazole derivatives exhibit highly surface area of 1845 m^2 g^{-1} and a carbon dioxide uptake ability of 4.63 mmol g^{-1} at 1.13 bar and 273 K.

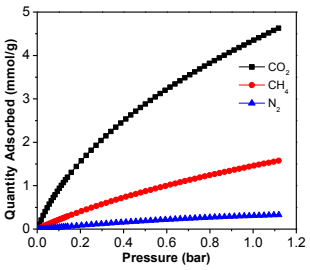

Xiao Yang, Miao Yu, Yang Zhao, Chong Zhang, Xiaoyan Wang, Jia-Xing Jiang*

Hypercrosslinked Microporous Polymers Based on Carbazole for Gas Storage and Separation